International Journal of Engineering Innovation & Research
Volume 9, Issue 5, ISSN: 2277 – 5668

Research on Shear Fracture Criterion of Advanced High Strength Dual Phase Steels

Qiutao Fu, Di Li*, Mengdi Li and Kaidi Wang
School of Transportation and Vehicle Engineering, Shandong University of Technology, Zhangdian, Zibo city, Shandong Province, P.R. China, 255049.
*Corresponding author email id: hahali@sdut.edu.cn

Date of publication (dd/mm/yyyy): 21/10/2020

***Abstract* – The universal ductile fracture criterion (such as the forming limit diagram (FLD)) cannot accurate predict the fracture of advanced high-strength dual-phase steels due to its unique shear fracture phenomenon. Based on the modified Mohr-Coulomb (MMC), this paper designs a series of high-strength Dual-Phase Steel (DP780) shear experiments, obtain the load-displacement curve and the stress triaxiality of the shear specimens at different angles, and the shear fracture strain-stress triaxiality curve is fitted to establish the shear fracture criterion, the curve model of shear fracture strain-stress triaxiality was further verified by the comparison between the tensile-bending test and the tensile-bending numerical simulation.**

***Keywords* – Advanced High Strength Dual-Phase Steels, Shear Experiments, Stress Triaxiality, Tensile-bending Forming, Numerical Simulation.**

I. INTRODUCTION

In recent years, advanced high-strength dual-phase (AHSDP) steel sheets are increasingly used in automobile companies due to its higher strength and good plasticity. Compared with ordinary deep-drawn steels, dual-phase (DP) steels have a lower yield ratio, the higher initial work hardening rate and good ductility, but the unique shear fracture mode of DP steels are significantly different from the local necking fracture of medium carbon steels and low alloy high strength steels. The widely used forming limit diagram (FLD) in sheet metal forming cannot accurately predict the shear fracture mode of DP steels, and an accurate ductile fracture criterion to predict its fracture still needs further research and development.

With the development of advanced high-strength steels, some criterions have been proposed to be applied to predict the shear fracture of DP steel plates. S.I. Oh [1] studied the effects of maximum tensile stress and equivalent stress factors, and proposed a regularized Crockroft & Latham fracture criterion. Yu Zhongqi [2] considered the effect of equivalent plastic strain on the development and change of holes and proposed a new ductile fracture criterion. It was believed that the result predicted by the ductile fracture criterion was better than the forming limit curve. The Jonson-cook [3] criterion introduces the influence of stress triaxiality on the failure strain, which is widely used in various softwares. Han Meng [4] explored the relationship between critical void volume fraction and stress triaxiality during necking fracture.

Lv Qinglong [5] established the prediction criterion for shear fracture of advanced high-strength DP steels based on Hill'48-MMC proposed by Bao[6] and Wierzbicki [7], and discussed some impact of key parameters changes on the shear fracture of DP590. Based on the modified Mohr-Coulomb fracture criterion, this paper designs a series of tensile shear experiments to explore the relationship between stress triaxiality and fracture strain under shear conditions. The stretch-bending simulation of shear fracture further verified the applicable scope of the MMC criterion.

II. Modified Mohr-Coulomb Criterion

Combining Hil1'48 yield criterion and MMC failure model, the Hil1' 48-MMC damage model were established to simulate the shear fracture of DP steel sheets. Based on the damage model, the Abaqus subroutine VUMAT was established, laying a solid foundation for the simulation of advanced high-strength DP steels.

The modified Mohr-Coulomb failure criterion was obtained by fitting the tensile and shear Mohr-Coulomb failure criterion [8].

$$F = \sigma_m \sin\phi + \sqrt{\overline{\sigma}^2 K^2(\theta) + m^2 c^2 \cos^2\phi} - c\cos\phi \tag{1}$$

where c and ϕ are symbols in geotechnical mechanics, the cohesive force and the angle of internal friction, respectively, while in this paper represents the shear strength of metal, σ_m denotes the average stress, $\overline{\sigma}$ is the equivalent stress, I_1 is the first invariant of stress. J_2 represent the first invariant of stress, θ is the Lode Angle, and m denotes the adjustment parameter.

The yield surface was optimized according to the modified Mohr-Coulomb failure criterion, In order to make the optimization result closer to the Mohr-Coulomb yield surface, a piecewise function is used to express $K(\theta)$, The piecewise function formula is as follows:

$$K(\theta) = \begin{cases} (A - B\sin 3\theta), & |\theta| > \theta_T \\ (\cos\theta - \frac{1}{\sqrt{3}}\sin\phi\sin\phi), & |\theta| < \theta_T \end{cases} \tag{2}$$

$$A = \frac{1}{3}\cos\theta_T \left(3 + \tan\theta_T \tan 3\theta_T + \frac{1}{\sqrt{3}}\text{sign}(\theta) \left(\tan 3\theta - 3\tan\theta_T \right) \sin\phi \right) \tag{3}$$

$$B = \frac{1}{3\cos 3\theta_T} \left(\text{sign}(\theta) \sin\theta_T + \frac{1}{\sqrt{3}}\sin\phi\cos\theta_T \right) \quad \text{sign}(\theta) = \begin{cases} 1, & \theta \geq 0^\circ \\ -1, & \theta < 0^\circ \end{cases} \tag{4}$$

where $\theta_T = 25^\circ$ was use in the literature [8].

Under macroscopic mechanics, the modified Mohr-Coulomb failure criterion formula is as follows:

$$D = \int_0^{\overline{\varepsilon_f}} \frac{d\overline{\varepsilon_p}}{\widehat{\varepsilon_f}(\eta,\bar{\theta})} = C = 1 \tag{5}$$

Where D is the damage index; $\widehat{\varepsilon_f}(\eta,\bar{\theta})$is the weight function, which is called the fracture envelope. Bai and Wierzbicki [8] deduced the formula of the fracture envelope of MMC:

$$\widehat{\varepsilon_f} = \left\{ \frac{A}{c_2} \left[c_3 + \frac{\sqrt{3}}{2-\sqrt{3}}(1-c_3)\left(\sec\left(\frac{\bar{\theta}\pi}{6}\right) - 1\right) \right] \times \left[\sqrt{\frac{1+c_1^2}{3}}\cos\left(\frac{\bar{\theta}\pi}{6}\right) + c_1\left(\eta + \frac{1}{3}\sin\left(\frac{\bar{\theta}\pi}{6}\right)\right) \right] \right\}^{-\frac{1}{n}} \tag{6}$$

When the external load presses proportional loading under the conditions, the fracture strain is the function of the stress triaxiality η and Rhodes Angle $\bar{\theta}$; A and n are swift hardening parameters; c_1, c_2 and c_3 are three material constants that are measured experimentally.

III. Shear Experiments

In order to study the relationship between low-stress triaxiality and fracture strain, at the same time, in order to obtain the change of stress triaxiality during the transition from the pure shear stress state to the unidirectional tensile stress state, it is necessary to conduct a series of shear experiments. The specific size of the shear experi-

-ment piece is designed as shown in Fig. 1.

In order to obtain the change of the stress field when the pure shear state transitions to the single tension state, refer to the literature [9], this paper designed the following sets of experiment pieces, the angle of the notch is 0°, 30, °45°, 60°, 90°, and the size is shown as follows:

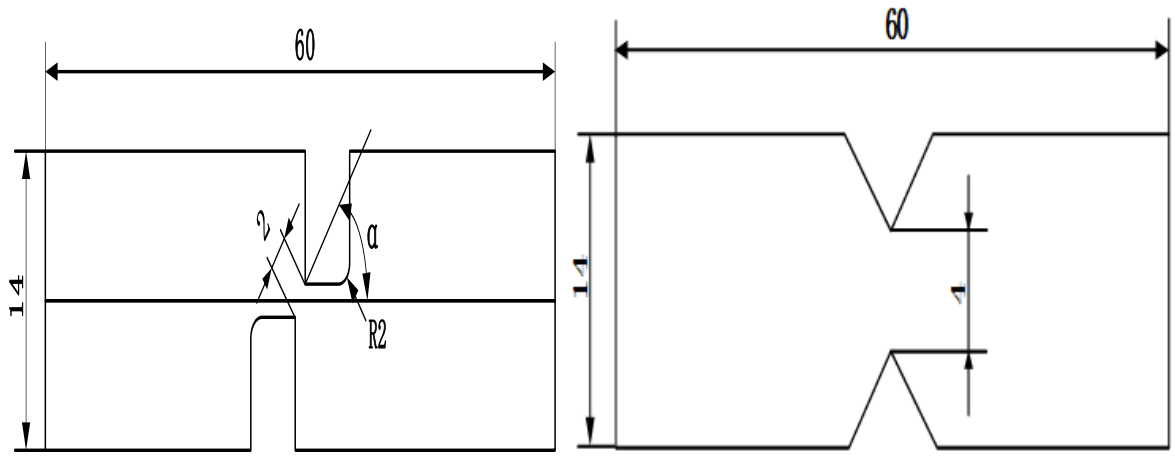

(a) α = 0, 30, 45, 60 degree specimens/mm (b) 90 degree specimen/mm

Fig. 1. Shear specimens dimensions.

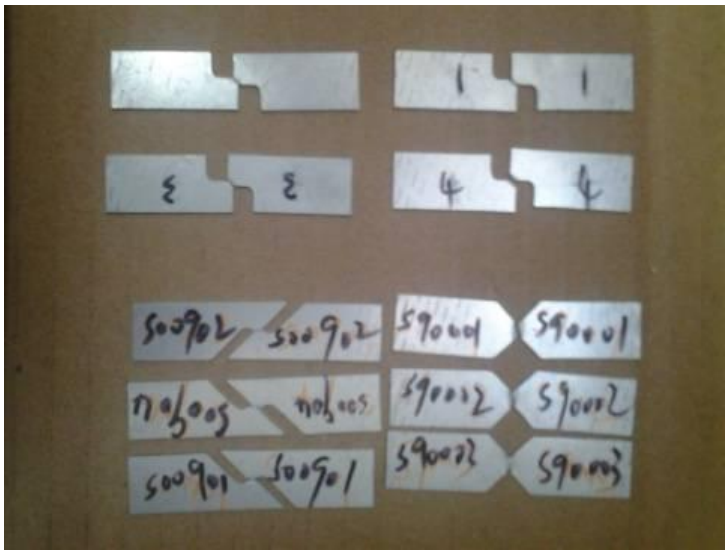

Fig. 2. Fracture diagram of shear specimen.

The tensile-shear experiment was performed on the SANS 30-ton universal testing machine in the laboratory, and the partially fractured specimens obtained are shown in Fig. 2. During the experiment, the ligament area in the middle of the shear specimen is subjected to parallel and intersecting tensile forces. The piece undergoes shearing dislocation, and with the continuous accumulation of plastic deformation, the fracture size continues to expand until it finally breaks.

Since the shear specimen has a certain slip during the stretching process of the stretching machine, and the stress state at the different angle gaps has both the shear stress and the axial tensile stress, the test machine obtains the stress-strain curve cannot reflect the true stress-strain curve relationship. The load-displacement curve should be used. The load-displacement curve fitted by shear simulation is shown as follows.

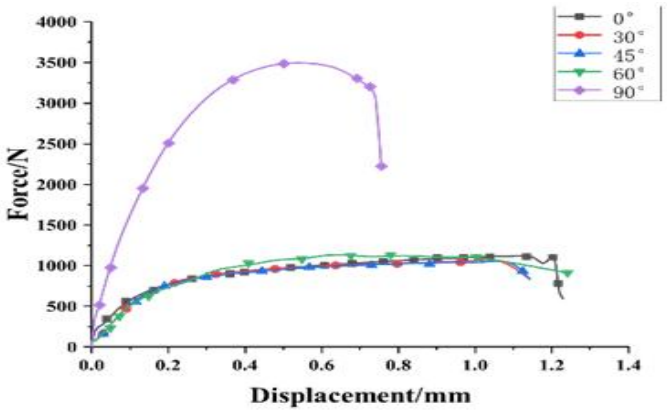

Fig. 3. Shear specimen load-displacement curve.

Fig. 3. shows the load-displacement curve of the shear specimen. The shear specimen does not have a yield platform. The curves obtained by different groups of experiments are similar. The load-displacement curves of the same group of materials have certain differences. There is not much difference in the value of displacement when it is generated.

IV. Fracture Characteristics under Combined Yension and Shear Deformation

4.1. *Method for Determining Stress Triaxiality*

The formula of stress triaxiality is as follows:

$$\eta = \frac{\sigma_m}{\bar{\sigma}} = \frac{(\sigma_1+\sigma_2+\sigma_3)/3}{\frac{1}{\sqrt{2}}\sqrt{(\sigma_1-\sigma_2)^2+(\sigma_2-\sigma_3)^2+(\sigma_1-\sigma_3)^2}} \tag{7}$$

where σ_1,σ_2,σ_3, represent the three principal stresses, σ_m is the hydrostatic stress (average stress), $\bar{\sigma}$ represents the Mises stress.

4.2. *Numerical Simulation*

The stress state at the fracture is obtained by finite element simulation, and the load-displacement curve got by the finite element simulation is compared with the load-displacement curve measured in the actual experiment to ensure that the curves are in good agreement. By obtaining the stress triaxial at the notch of the shear specimen Degree change curve, the relationship curve between stress triaxiality and ultimate fracture strain in the low-stress triaxiality state is obtained.

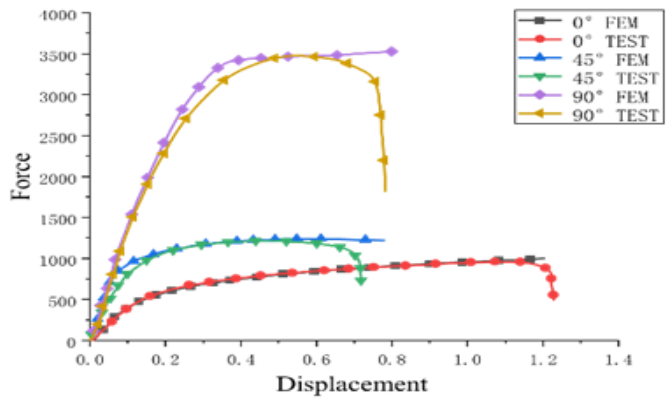

Fig. 4. Fitting diagram of load-displacement curve.

Fig. 4 is the load-displacement curve measured by the experiment of different angle specimens and the load-displacement curve that are simulated and corrected by software. The results are in good agreement. Compared with the actual value, the error is small. Employing finite element model with high accuracy, the stress triaxiality and fracture strain simulated here can better reflect the change of the material's stress field in actual deformation.

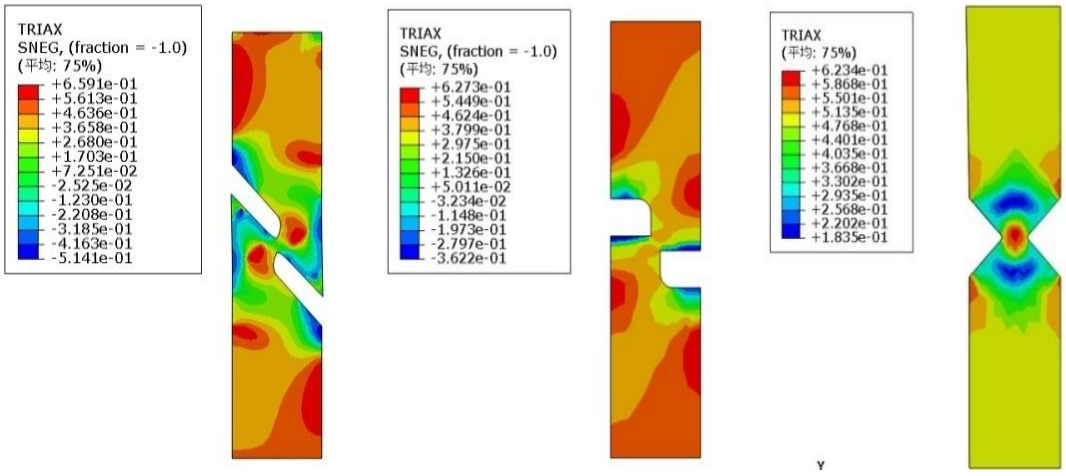

Fig. 5. Stress triaxiality cloud diagram.

Fig. 5. is the corresponding stress triaxiality diagram. It can be seen that the stress triaxiality from the 0° specimen to the 90° specimen notch is constantly increasing, indicating that the stress state is the transition from pure shear state to single tension status. And fracture is easy to occur in the position with greater stress, which shows that the simulation result is consistent with the fracture result of the actual experimental shear specimen in Fig. 2.

4.3. *The Relationship between Fracture Strain and Stress Triaxiality Under Shear*

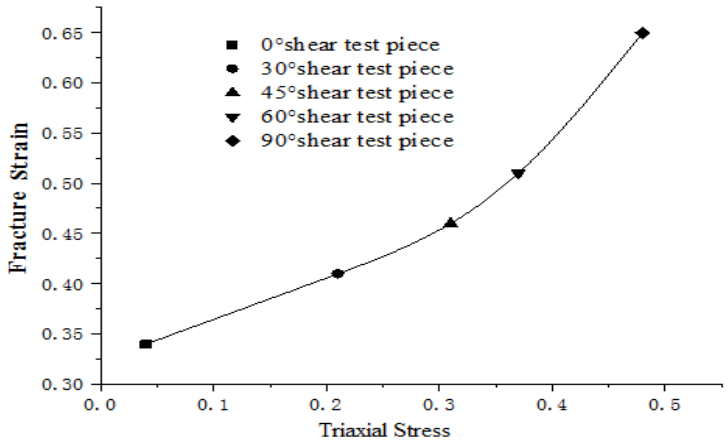

Fig. 6. shear fracture strain-stress triaxiality curve.

Fig. 6 represents the shear fracture strain-stress triaxiality curve, which shows the relationship between the fracture strain and the stress triaxiality of the specimens sheared at different angles. As the stress triaxiality increases, the fracture strain tends to increase, which is a monotonically increasing function. The fitting curve is as follows:

$$\varepsilon_f = c_1 + c_2 * \eta^2 \quad (8)$$

where c_1 =0.3423, c_2 = 1.368. Two parameters c_1 and c_2 can be determined with two kinds of shear experiments in Fig. 1.

V. EXAMPLES

In order to prove that the MMC criterion can predict the forming limit of DP steels, a series of tensile-bending experiments are carried out to verify it, the fracture diagram of tensile-bending specimens with different fillet radius are in Fig. 7, the punch radius are 1mm, 4mm, 5mm, and the fracture modes are shear fracture.

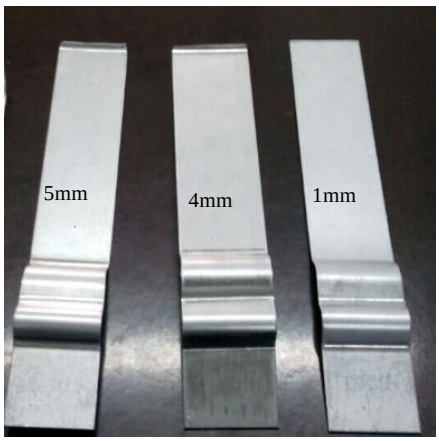

Fig. 7. Fracture modes of DP780 at different radius.

The custom MMC criterion model in ABAQUS VUMAT simulates the result of DP780 pull-bending forming with a small fillet radius. The stretch-bending forming model is shown in Fig. 8. The fillet radius at the entrance of the die is Rd1 = 5mm, and the punch radius Rp = 1mm, Mold gap G = 1.2 mm.

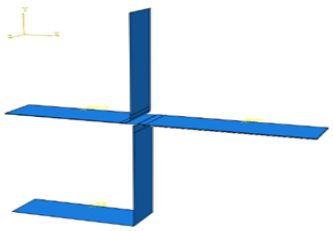

Fig. 8. FE model for trough stamping forming.

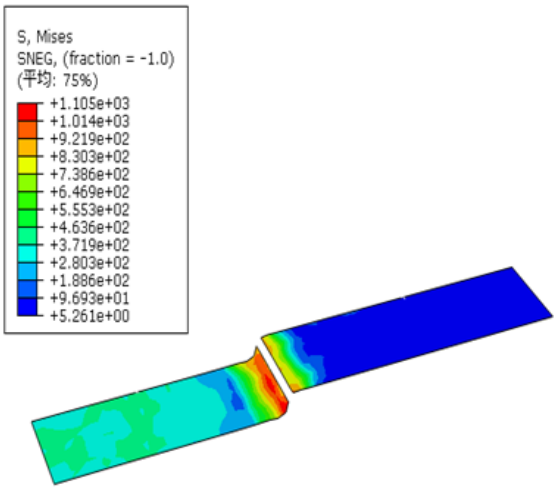

Fig. 9. MMC Mises stress cloud map.

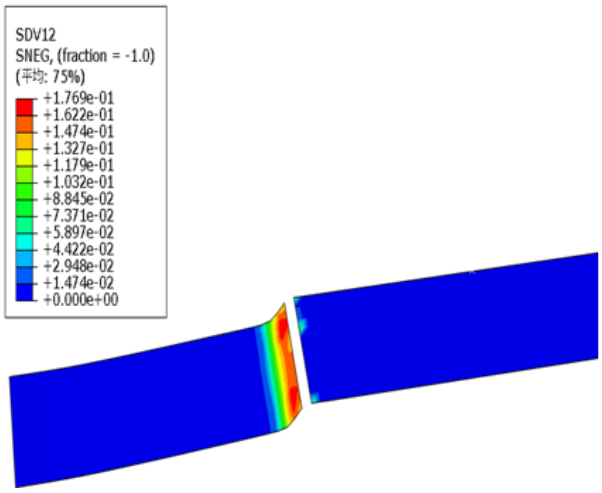

Fig. 10. MMC Equivalent plastic strain.

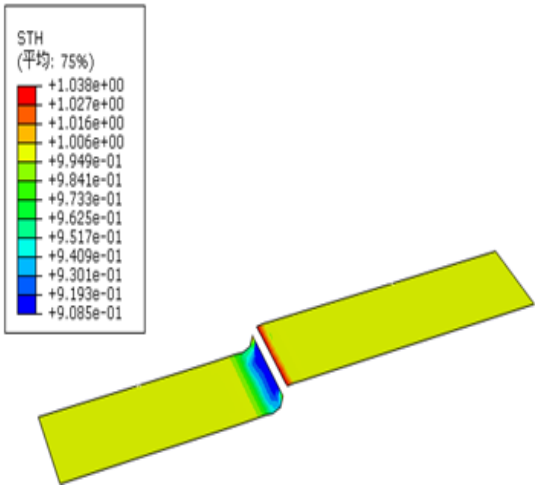

Fig. 11. MMC thickness distribution.

From the stress cloud diagram in Fig. 9, it can be seen that the DP steels bending simulation using the MMC criterion broke at the small corner radius of the die, and it can be observed that the stress here is not the maximum value. Fig. 10 is the MMC Equivalent plastic strain. According to the plastic strain, it can be seen that there is no obvious thinning and necking at the fracture position of the sheet under the MMC criterion. The thickness distribution diagram of Fig. 11 shows that the thinning rate under the MMC criterion is about 9%, which proves that the shear fracture does not have obvious thinning and necking characteristics.

VI. Conclusion

Based on the modified Mohr-Coulomb criterion, this paper designs a series of high-strength steel DP780 shear experiments at different angles, and obtains the load-displacement curves of the shear experiments, the relationship between stress triaxiality and ultimate fracture strain is obtained by simulating the triaxial stress curve at the notch of the shear specimen, and the shear fracture criterion is obtained by fitting the curve, the fracture criterion has two parameters, which are obtained from two different angles shear fracture experiments. Combing tensile-bending experiments on specimens with different fillet radius and numerical simulation of shear-fracture stretch-bending forming process, which verified the curve model of shear fracture strain-stress triaxiality and proved the effectiveness of MMC.

Acknowledgements

The present research was supported by the Shandong Provincial Natural Science Foundation (ZR2010EL 002).

References

[1] OhS I, Chen C.C., Kobayashi S. Ductile fracture in ax-symmetric extrusion and drawing [J]. Journal of Engineering for Industry, Transaction of the ASME, 1979, 101 (1):23-44.
[2] Zhongqi Yu, Yuying Yang, Yongzhi Wang, et al. Prediction of forming limit of aluminum alloy sheet based on ductile fracture criterion [J]. China Nonferrous Metals Journal of metals, 2003, 13(5): 1223-1226.
[3] Johnson G.R., Cook W.H. Fracture characteristics of three metals subjected to various strains, strain rates, temperatures and pressures [J]. Engineering Fracture Mechanics, 1985, 21(1): 31-42.
[4] Meng Han, Di Li, Caifeng Sun, et al. Research on fracture failure criterion of dual-phase steel based on modified GTN model [J]. Chinese Journal of Plasticity Engineering, 2020, 27(01): 117-122.
[5] Qinglong LYU, Caifeng Sun, Lianxing Zhao, Di Li. Simulation of tensile bending shear fracture of advanced high strength duplex steel body plate based on VUMAT [J]. Agricultural equipment and vehicle engineering, 2015, 53(4): 36-40.
[6] Bao, Y.B., 2003. Prediction of ductile crack formation in uncracked bodies [D]. PhD Thesis, Massachusetts Institute of Technology.
[7] Bai, Y., Wierzbicki, T., 2008. A new model of metal plasticity and fracture with pressure and Lode dependence [J]. International Jour-

-nal of Plasticity 24, 1071–1096.
[8] Shanpo Jia, Weizhong Chen, Jianping Yang, Peishuai Chen. An elastoplastic constitutive model based on modified Mohr-Coulomb criterion and its numerical implementation [J]. Rock and soil mechanics, 2010, 31(07): 2051-2058.
[9] Jien Chen. Study on material failure based on stress triaxial degree [D]. Hubei: Huazhong University of Science and Technology, 2012.

AUTHOR'S PROFILE

First Author
Qiutao Fu, Master in reading, Male, School of Transportation and Vehicle Engineering, Shandong University of Technology, Zhangdian, Zibo city, Shandong Province, P.R. China, 255049. email id: 747390327@ qq. com

Second Author
Di Li*, Male, Doctor of Engineering, Associate professor, School of Transportation and Vehicle Engineering, Shandong University of Technology, Zhangdian, Zibo city, Shandong Province, P.R. China, 255049 (Correspondence author).
email id: hahali@ sdut.edu.cn

Third Author
Mengdi Li, Male, Master in reading, School of Transportation and Vehicle Engineering, Shandong University of Technology, Zhangdian, Zibo city, Shandong Province, P.R. China, 255049.

Fourth Author
Kaidi Wang, Male, Master in reading, School of Transportation and Vehicle Engineering, Shandong University of Technology, Zhangdian, Zibo city, Shandong Province, P.R. China, 255049.